

# Functional Analysis of SPINDLY in Gibberellin Signaling in Arabidopsis<sup>1[C][W][OA]</sup>

Aron L. Silverstone<sup>2,3</sup>, Tong-Seung Tseng<sup>2,4</sup>, Stephen M. Swain<sup>5</sup>, Alyssa Dill, Sun Yong Jeong, Neil E. Olszewski, and Tai-ping Sun\*

Department of Biology, Duke University, Durham, North Carolina 27708 (A.L.S., A.D., S.Y.J., T.-p.S.); and Department of Plant Biology, University of Minnesota, St. Paul, Minnesota 55108 (T.-S.T., S.M.S., N.E.O.)

The Arabidopsis (*Arabidopsis thaliana*) SPINDLY (SPY) protein negatively regulates the gibberellin (GA) signaling pathway. SPY is an O-linked N-acetylglucosamine (GlcNAc) transferase (OGT) with a protein-protein interaction domain consisting of 10 tetratricopeptide repeats (TPR). OGTs add a GlcNAc monosaccharide to serine/threonine residues of nuclear and cytosolic proteins. Determination of the molecular defects in 14 new *spy* alleles reveals that these mutations cluster in three TPRs and the C-terminal catalytic region. Phenotypic characterization of 12 *spy* alleles indicates that TPRs 6, 8, and 9 and the catalytic domain are crucial for GA-regulated stem elongation, floral induction, and fertility. TPRs 8 and 9 and the catalytic region are also important for modulating trichome morphology and inflorescence phyllotaxy. Consistent with a role for SPY in embryo development, several alleles affect seedling cotyledon number. These results suggest that three of the TPRs and the OGT activity in SPY are required for its function in GA signal transduction. We also examined the effect of *spy* mutations on another negative regulator of GA signaling, REPRESSOR OF *ga1-3* (RGA). The DELLA motif in RGA is essential for GA-induced proteolysis of RGA, and deletion of this motif (as in *rga-Δ17*) causes a GA-insensitive dwarf phenotype. Here, we demonstrate that *spy* partially suppresses the *rga-Δ17* phenotype but does not reduce *rga-Δ17* or RGA protein levels or alter RGA nuclear localization. We propose that SPY may function as a negative regulator of GA response by increasing the activity of RGA, and presumably other DELLA proteins, by GlcNAc modification.

GAs are tetracyclic diterpenoid compounds that affect many aspects of plant growth and development, including seed germination, stem elongation, flowering, and fruit and seed development (for review, see Olszewski et al., 2002; Sun and Gubler, 2004; Fleet and Sun, 2005; Swain and Singh, 2005). In Arabidopsis (*Arabidopsis thaliana*), *spindly* (*spy*) mutants were first identified by virtue of their resistance to both the

germination inhibiting and dwarfing effects of paclobutrazol, a gibberellin (GA) biosynthesis inhibitor (Jacobsen and Olszewski, 1993). All the known *spy* alleles are recessive and exhibit some phenotypes similar to those of wild-type plants repeatedly treated with GA (Jacobsen and Olszewski, 1993). To varying degrees, *spy* mutants also suppress all of the phenotypes caused by GA deficiency (Jacobsen and Olszewski, 1993; Silverstone et al., 1997). Therefore, SPY has been hypothesized to negatively regulate GA signal transduction. However, not all of the *spy* mutant phenotypes (e.g. altered phyllotaxy) mimic wild-type plants that are overdosed with GA, indicating that SPY regulates additional cellular pathways (Swain et al., 2001, 2002; Tseng et al., 2004; Greenboim-Wainberg et al., 2005).

SPY encodes a 104-kD peptide with similarity to O-linked N-acetylglucosamine (GlcNAc) transferase (OGT) from human, rat, and *Caenorhabditis elegans* (Jacobsen et al., 1996; Kreppel et al., 1997; Lubas et al., 1997), and SPY expressed in insect cells possesses OGT activity (Thornton et al., 1999). Both SPY and animal OGTs contain multiple copies of N-terminal tetratricopeptide repeats (TPR). TPR motifs are highly degenerate 34-amino acid repeats with eight loosely conserved residues (Blatch and Lässle, 1999). TPRs are usually present in multiple copies and act as scaffolds for assembly of multiprotein complexes with specific blocks of TPR motifs mediating the interaction with different proteins (Tzamarias and Struhl, 1995; Moir

<sup>1</sup> This work was supported by the National Science Foundation (grant nos. IBN-9723171, IBN-0078003, and IBN-0348814 to T.-p.S. and grant nos. MCB-9604126, MCB-9983583, and MCB-0112826 to N.E.O.).

<sup>2</sup> These authors contributed equally to the paper.

<sup>3</sup> Present address: Syngenta Biotechnology, Inc., 3054 Cornwallis Rd., Research Triangle Park, NC 27709.

<sup>4</sup> Present address: Carnegie Institution of Washington, Department of Plant Biology, 260 Panama St., Stanford, CA 94305.

<sup>5</sup> Present address: CSIRO Plant Industry, Private Mail Bag, Merbein, VIC 3505, Australia.

\* Corresponding author; e-mail tps@duke.edu; fax 919-613-8177.

The author responsible for distribution of materials integral to the findings presented in this article in accordance with the policy described in the Instructions for Authors ([www.plantphysiol.org](http://www.plantphysiol.org)) is: Tai-ping Sun (tps@duke.edu).

<sup>[C]</sup> Some figures in this article are displayed in color online but in black and white in the print edition.

<sup>[W]</sup> The online version of this article contains Web-only data.

<sup>[OA]</sup> Open Access articles can be viewed online without a subscription.

[www.plantphysiol.org/cgi/doi/10.1104/pp.106.091025](http://www.plantphysiol.org/cgi/doi/10.1104/pp.106.091025)

et al., 1997; Ollendorff and Donoghue, 1997; Young et al., 1998). The crystal structure of the TPR domain of human OGT indicates that, like other TPR proteins, each TPR is composed of one pair of  $\alpha$  helices, which are packed in an antiparallel arrangement to the neighboring helices, with the domain folded into a right-handed superhelix (Jinek et al., 2004). The TPR motifs of SPY and animal OGT mediate protein-protein interactions that are important for both the substrate specificity and the assembly of the enzyme (Kreppel and Hart, 1999; Lubas and Hanover, 2000; Tseng et al., 2001, 2004). Protein interactions at the TPR domain are likely to be important for GA signaling, because ectopic expression of the SPY TPR domain alone causes changes in GA response (Tseng et al., 2001).

The C terminus of OGT is the catalytic domain. Two conserved domains (CDI and CDII) are present in the C termini of SPY and animal OGTs (Fig. 1A). Mutational analysis suggests that CDI and CDII are part of a UDP-GlcNAc binding pocket and participate in the transfer of GlcNAc (Lazarus et al., 2005).

OGTs transfer a GlcNAc monosaccharide in O-linkage to Ser/Thr of nuclear and cytosolic proteins (Love and Hanover, 2005). In animals, the modification is believed to regulate diverse processes. More than 100 O-GlcNAc modified proteins have been identified. These proteins include regulatory proteins, enzymes, and structural proteins. Many of the proteins are phosphoproteins, and in some cases, O-GlcNAc modification and phosphorylation can occur at the same site (Comer and Hart, 2001; Wells et al., 2001; Slawson and Hart, 2003; Love and Hanover, 2005).

While animals have a single OGT gene, Arabidopsis contains a second OGT gene (*SECRET AGENT [SEC]*; Hartweck et al., 2002). Although *sec* plants do not exhibit dramatic defects, the *spy sec* double mutant has an embryo-lethal phenotype. Deleting the mouse OGT gene also causes lethality (Shafi et al., 2000). Interestingly, loss of OGT activity does not cause lethality in *C. elegans* (Hanover et al., 2005).

In addition to SPY, the DELLA proteins (REPRESSOR OF *gai-3* [RGA], GA INSENSITIVE [GAI], RGA-LIKE1 [RGL1], and RGL2) are also negative regulators of GA signaling in Arabidopsis (Olszewski et al., 2002; Peng and Harberd, 2002). The DELLA proteins are thought to be nuclear transcriptional regulators. RGA and GAI play a major role in repressing stem elongation and floral induction (Dill and Sun, 2001; King et al., 2001), and RGL2 is important in inhibiting seed germination (Lee et al., 2002), whereas a combination of RGA, RGL1, and RGL2 modulates floral development (Cheng et al., 2004; Tyler et al., 2004; Yu et al., 2004). It has been demonstrated that GA derepresses its signaling pathway by inactivating the DELLA proteins, and the conserved DELLA motif, which is located near the N terminus of these proteins, is required for GA-dependent proteolysis of these repressors (Sun and Gubler, 2004). GA has been shown to induce degradation of RGA, GAI, and RGL2 (Silverstone et al., 2001; Dill et al., 2004; Tyler et al., 2004), and mutant

alleles (*gai-1*, *rga- $\Delta$ 17*, and *rgl1- $\Delta$ 17*) that encode DELLA-motif deleted mutant DELLA proteins confer a GA-insensitive dwarf phenotype (Peng et al., 1997; Dill et al., 2001; Wen and Chang, 2002). This proteolysis event is likely to be targeted by a ubiquitin E3 ligase complex SCF<sup>SLY1</sup> to the 26S proteasome (McGinnis et al., 2003; Dill et al., 2004; Fu et al., 2004; Tyler et al., 2004). The DELLA proteins and their function in GA signaling are conserved in plants (Thomas and Sun, 2004). For example, the DELLA proteins in barley (*Hordeum vulgare*; SLN1) and in rice (*Oryza sativa*; SLR1) are also GA signaling repressors and are responsive to GA-induced degradation by the ubiquitin-proteasome pathway (Fu et al., 2002; Gubler et al., 2002; Itoh et al., 2002; Sasaki et al., 2003). Mutations in the DELLA motif of SLN1 and SLR1 also confer GA-insensitive dwarf phenotypes. Recently, the rice *GID1* protein and its Arabidopsis orthologs (*AtGID1a*, *AtGID1b*, and *AtGID1c*) have been shown to function as GA receptors (Ueguchi-Tanaka et al., 2005; Nakajima et al., 2006). In the presence of bioactive GA, *GID1* interacts with DELLA proteins in yeast (*Saccharomyces cerevisiae*) two-hybrid assays, suggesting that a GA-*GID1*-DELLA complex may be targeted for degradation by the SCF<sup>SLY1/GID2</sup> complex.

The relationship between the DELLA proteins and SPY in GA signaling is not clear. The DELLA proteins contain sequences that are rich in Ser and Thr residues, which may be target sites for OGT (Peng et al., 1997; Silverstone et al., 1998). Therefore, SPY may activate the DELLA proteins by GlcNAc modification, which has been shown in animal systems to affect nuclear localization, protein stability, and/or activity of target proteins (Love and Hanover, 2005). Consistent with this model, the dwarf phenotype of the gain-of-function *gai-1* mutant is largely suppressed by *spy* alleles (Wilson and Somerville, 1995; Jacobsen et al., 1996; Peng et al., 1997).

Previously, the mutations of five *spy* alleles have been identified by DNA sequence analysis (Jacobsen et al., 1996). More *spy* alleles have been isolated through suppressor screens of the *gai-3* and *gai-1* mutants (Carol et al., 1995; Wilson and Somerville, 1995; Silverstone et al., 1997). Here, we report the characterizations of 15 new *spy* alleles. Identifying the mutations in *spy* alleles helped us define the putative functional motifs of the SPY protein and the significance of these motifs in regulating pathways related and unrelated to GA signal transduction. We also showed that, similar to *gai-1*, the phenotypes of *rga- $\Delta$ 17* were partially suppressed by a *spy* allele. The *spy* mutation does not cause a reduction in *rga- $\Delta$ 17* or RGA protein levels, nor does it alter the nuclear localization of these proteins, suggesting that SPY may increase the activity of the RGA protein.

## RESULTS

The *spy* mutants exhibit pleiotropic phenotypes, some of which are related to elevated GA response

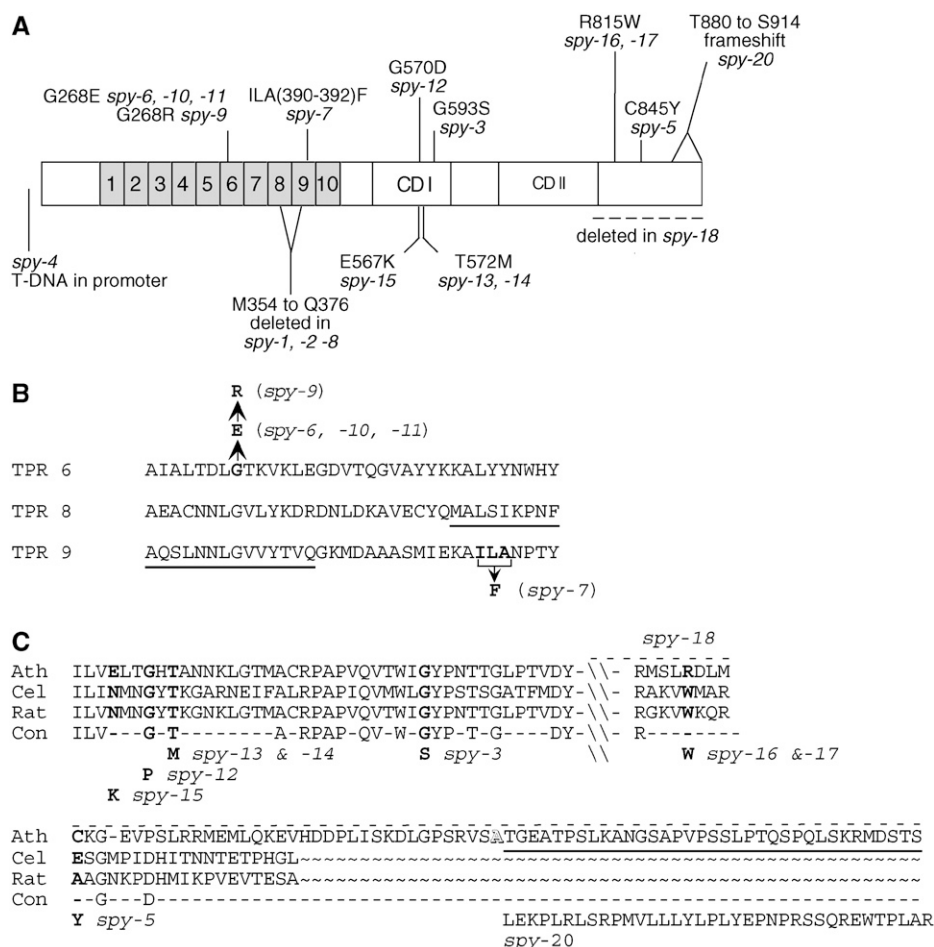


**Figure 1.** The protein defects caused by 19 *spy* alleles. A, Schematic representation of the SPY protein with the nature and location of 19 *spy* mutations indicated. The numbered boxes represent the TPRs. CD I and CD II are conserved domains found in OGTs (Roos and Hanover, 2000). The dotted line indicates the portion of SPY encoded by the *Pst*I fragment affected in *spy-18*. The defects in *spy-1* to *spy-5* were determined previously (Jacobsen et al., 1996). B, Locations of the mutations affecting TPRs 6, 8, and 9. The underlined amino acids of TPR 8 and 9 are predicted to be deleted in *spy-1*, *spy-2*, and *spy-8*. *spy-7* causes replacement of the bolded amino acids with Phe. C, C-terminal alignment of SPY (Ath) and OGTs from *C. elegans* (Cel) and rat (Rat). Consensus residues (Con) represent conserved amino acids among the three sequences. The amino acid changes caused by the *spy* alleles are indicated below the consensus. The portion of SPY encoded by the *Pst*I fragment that was affected in *spy-18* is indicated by the dotted line above the SPY sequence. The *spy-20* mutation deleted one nucleotide of codon 879 (Table I), which affects the amino acids after Ala-879 (underlined). The new amino acids encoded by the frame-shifted region are shown below the consensus. Due to a single nucleotide polymorphism, position 879, A, is an Ala in *Ler* and Ser in *Col-0*.

(early floral induction, reduced fertility, and increased trichome branching), but others are not (such as altered phyllotaxy, cytokinin response, light responses, and circadian rhythms, and reduced hypocotyl and rosette growth; Thornton et al., 1999; Swain et al., 2001; Tseng et al., 2004; Greenboim-Wainberg et al., 2005). To determine the functional motifs in SPY and identify new *spy* phenotypes, we identified 13 new recessive *spy* alleles (*spy-8–spy-20*) that suppress dwarfism caused by GA deficiency (see “Materials and Methods”). The mutations responsible for 12 of these alleles and two previously identified alleles were determined. The GA signaling defects of 10 of the new mutants and two previously characterized mutants were compared. In addition, these mutants were examined for new phenotypes.

### Characterization of Molecular Defects of *spy* Alleles

The transcribed portion of the *SPY* locus (At3g11540) contains 18 exons and 17 introns that span 5.8 kb. We first attempted to map the mutations of some of the *spy* alleles by examining restriction digests of PCR products of the exons of these alleles for single-stranded conformational polymorphisms (SSCP; Hayashi, 1992; Bailey, 1995). SSCPs were detected in exon 9 of *spy-7*, exon 13 of *spy-13* and *spy-14*, and exon 18 of *spy-16* and *spy-17* (data not shown). DNA sequencing confirmed that each of the exons exhibiting a SSCP contained a mutation (Table I; Fig. 1). SSCPs were not detected in any of the exons of *spy-6*, *spy-8*, *spy-9*, *spy-10*, *spy-11*, and *spy-15*.

The mutations of *spy-6*, *spy-8*, *spy-9*, *spy-10*, *spy-11*, *spy-12*, *spy-15*, *spy-18*, *spy-19*, and *spy-20* were investigated by sequencing their exons (Table I; Fig. 1). The mutations of *spy-6*, *spy-8*, *spy-9*, *spy-10*, and *spy-11* affected the N terminus of SPY, while *spy-12*, *spy-15*, and *spy-20* represented mutations in the C-terminal region of SPY (Fig. 1). The *spy-8* mutation is identical to that of *spy-1*, and the last G of exon 8 is mutated to an A. The *spy-1* mutation causes frequent missplicing and deletion of exon 8 (Jacobsen et al., 1996). Although this has not been confirmed experimentally, *spy-8* mRNA is expected to have the same splicing defect as *spy-1*. Skipping of exon 8 results in an in-frame deletion of Met-354 to Gln-376.

Hybridization of Southern blots containing restriction digests of *spy-18* genomic DNA (data not shown) indicated that the last *Pst*I fragment of the gene was missing (Fig. 1). With the exception of the last exon of the gene, all of the exons were amplified by PCR. Therefore, the deletion must begin within the last exon of the gene or the intron that precedes this exon. The extent of the deletion beyond the *SPY* locus has not been determined, but it must extend into the *Pst*I fragment following the gene, because that fragment was not detected. Based on this analysis, the deletion in *spy-18* could begin at Leu-782, the first amino acid encoded in this exon or somewhere downstream of this.

We did not detect any mutation in any of the exons in the *spy-19* locus by DNA sequence analysis. This mutant allele did not show visible deletions, insertions, or DNA arrangements around the *spy* locus by genomic DNA-blot analysis (data not shown). It is possible that the mutation is localized in the promoter or an intron.

### Phenotypic Characterization of the *spy* Alleles

To investigate the role of different domains of SPY in GA-related and unrelated functions, we analyzed and

compared the phenotypes of 12 *spy* mutants: *spy-2*, *-4*, *-8*, *-9*, *-11*, *-12*, *-14*, *-15*, *-16*, *-18*, *-19*, and *-20*. *spy-4* contains a T-DNA insertion that is 13 bp upstream of the *SPY* transcriptional start site, which greatly reduces the abundance of the *SPY* transcript (Jacobsen et al., 1996; Filardo, 2004). *spy-9* and *-11* affect TPR6, *spy-2* and *-8* result in partial deletion of TPR8 and TPR9, and *spy-12*, *-14*, *-15*, *-16*, *-18*, and *-20* encode *spy* proteins with missense or deletion mutations in the catalytic region. The unidentified mutation in *spy-19* is likely to be in the promoter or intron sequence. Most of these mutants (*spy-8* to *spy-20*) were isolated as suppressors of *ga1-3* in the Landsberg *erecta* (*Ler*) background (Silverstone et al., 1997, 1998). The homozygous *spy-8* to *spy-20* mutants (backcrossed once) were identified in the F<sub>2</sub> generation of crosses between the *spy ga1-3* double mutants and *Ler*. The *spy-2* (originally in Columbia [Col-0]) and *spy-4* (originally in Wassilewskija) mutants had been crossed for three or four generations, respectively, into *Ler* wild-type plants that were also included in these analyses for comparison.

The following sets of parameters were measured for these *spy* mutants and wild type: flowering time (in days and in leaf number), final stem height, number of siliques on the primary inflorescence stem, and the average number of seeds in the first 15 siliques as a measure of fertility. In addition, we noted any other developmental abnormalities, including alterations in phyllotaxy, trichome branching, and cotyledon number.

### Flowering Time

Flowering time can be measured both in days to flower (a chronological measurement) and developmental age, by scoring the number of both rosette and cauline leaves produced. Bioactive GAs are an essential part of the autonomous flowering pathway. The *ga1-3* mutant contains extremely low levels of GAs

**Table I.** Mutations of new *spy* alleles

Allele	DNA Mutation <sup>a</sup>	Protein Mutation	Mutagen	Background
<i>spy-6</i>	G (1823) → A	Gly-268 → Glu	EMS	Col-0
<i>spy-7</i>	ATACTTGC (2902–2909) → TT	Ile-Leu-Ala (390–392) → Phe	γ-Radiation	<i>Ler</i>
<i>spy-8</i>	G (2778) → A; skipping of exon 8 (2710–2788) <sup>b</sup>	Partial deletion of TPR8 → TPR9 (354–376)	EMS	<i>Ler</i>
<i>spy-9</i>	G (1822) → A	Gly-268 → Arg	EMS	<i>Ler</i>
<i>spy-10</i>	G (1823) → A	Gly-268 → Glu	EMS	<i>Ler</i>
<i>spy-11</i>	G (1823) → A	Gly-268 → Glu	EMS	<i>Ler</i>
<i>spy-12</i>	G (3893) → A	Gly-570 → Asp	EMS	<i>Ler</i>
<i>spy-13</i>	C (3899) → T	Thr-572 → Met	EMS	<i>Ler</i>
<i>spy-14</i>	C (3899) → T	Thr-572 → Met	EMS	<i>Ler</i>
<i>spy-15</i>	G (3883) → A	Glu-567 → Lys	EMS	<i>Ler</i>
<i>spy-16</i>	C (5076) → T	Arg-815 → Trp	EMS	<i>Ler</i>
<i>spy-17</i>	C (5076) → T	Arg-815 → Trp	EMS	<i>Ler</i>
<i>spy-18</i>	Deletion of 3' end <sup>c</sup>	Leu-782 to Ser-914 deleted	Fast neutron	<i>Ler</i>
<i>spy-19</i>	n.i. <sup>d</sup>	n.i.	Fast neutron	<i>Ler</i>
<i>spy-20</i>	T (5270) deleted	Frameshift of Thr-880 to Ser-914	Fast neutron	<i>Ler</i>

<sup>a</sup>The location of each mutation in SPY genomic DNA is indicated relative to the start of transcription (GenBank accession no. NM\_111987). <sup>b</sup>The *spy-8* mutation is predicted to cause missplicing leading to deletion of exon 8 from the mature mRNA and amino acids 354 to 376 from SPY. <sup>c</sup>The precise 5' end of the deletion is not known but could cause a deletion from Leu-782 to the end of SPY. <sup>d</sup>Not identified.

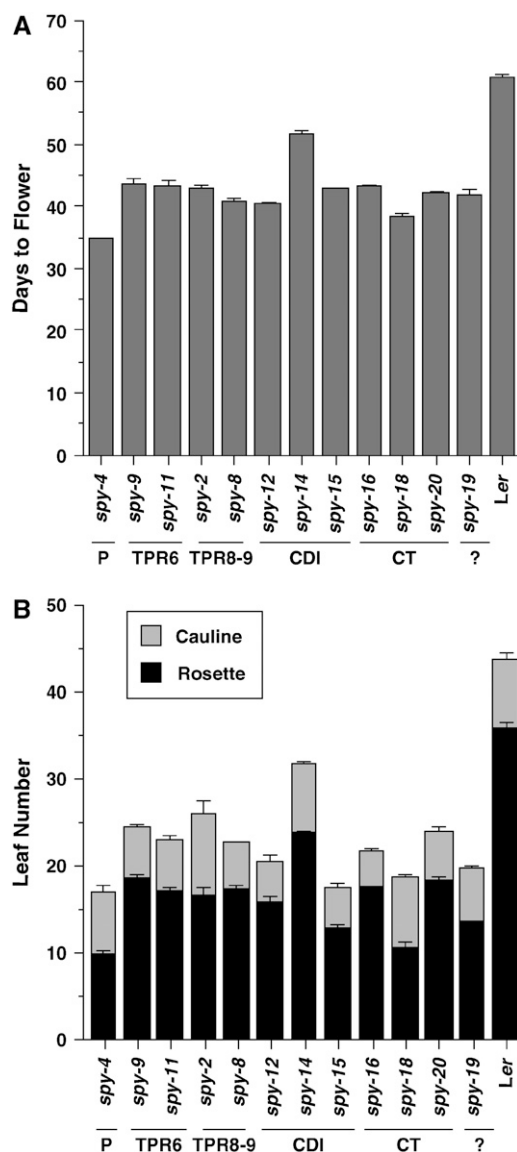


**Figure 2.** The *spy* alleles flowered earlier than wild type in SD. A, Number of days from sowing until floral buds are clearly visible. B, Number of rosette and cauline leaves produced by the primary inflorescence stem after bolting. The values plotted are the means  $\pm$  SE of 10 plants. Some error bars are too small to be seen. The *spy* alleles are organized in the order of the mutations in the *SPY* genomic sequence. P, Promoter; CT, C terminus.

(Silverstone et al., 2001) and flowers very late in long day (LD) and not at all under short day (SD) consisting of fluorescent light (Wilson et al., 1992). Thus, GA is required for floral induction in SD in *Arabidopsis* under specific laboratory conditions. In addition, GA also promotes the transition from vegetative-to-reproductive phase in LD. Several *spy* alleles (*spy-1* to *spy-5* in a wild-type background, and *spy-2* to *spy-4* and *spy-8* to *spy-9* in a *gal* background) confer an earlier flowering phenotype, consistent with the role of *SPY* as a negative regulator of GA signaling (Jacobsen and Olszewski, 1993; Jacobsen et al., 1996; Silverstone

et al., 1997; Swain et al., 2001). However, it has been proposed that *spy* alleles also promote flowering through action in the LD flowering pathway (Tseng et al., 2004).

In SD, we found that almost all of the *spy* alleles (except *spy-14*) flowered significantly earlier than wild type (17–23 d earlier with 18–28 fewer leaves; Fig. 2). The *spy-14* mutant only flowered 9 d earlier and produced 12 fewer leaves than wild type, indicating that this allele has a milder defect in repressing GA-promoted flowering. We also measured flowering time under LD conditions, and the results are similar, but with a smaller reduction in flowering time relative to wild type compared to SD (data not shown). These data indicated that TPRs 6, 8, and 9, CDI and the C terminus of *SPY* are all crucial for repressing floral induction.

### Fertility

Bioactive GAs are essential for flower development in *Arabidopsis*. The GA-deficient mutant *gal-3* is male sterile (Koornneef and van der Veen, 1980). This fertility defect can be partially rescued by derepression of the GA signaling pathway due to loss-of-function mutations in *SPY* or *DELLA* protein genes (Silverstone et al., 1997; Cheng et al., 2004; Tyler et al., 2004; Yu et al., 2004). However, an optimal concentration of GA is important. Whereas an absence of GA results in male sterility, an excess of GA or derepressed GA signaling also leads to partial-to-complete male sterility (Jacobsen and Olszewski, 1993; Dill and Sun, 2001). In LD, all the *spy* mutant lines had some degree of reduced fertility when measuring seeds/silique on the primary inflorescence, from a moderate lowering of between 50% and 70% of wild type in *spy-11*, *-14*, and *-20* to almost completely sterile in *spy-2*, *-18*, and *-19* (Fig. 3). However, *spy-2*, *-18*, and *-19* plants did produce a small amount of viable seeds from their axillary inflorescence stems. Day length appeared to have an effect on fertility. SD conditions were able to increase the fertility of most *spy* lines, although *spy-18* still remained highly infertile (Fig. 3).

As evident by the reduced fertility of *spy-2*, *-8*, *-9*, *-12*, *-16*, and *-18* mutations, TPRs 6, 8, and 9, and catalytic region are important for *SPY*'s function in regulating fertility. Interestingly, the C-terminal-most mutation, *spy-20*, did not have a large effect on this developmental process.

### Height

GA promotes stem elongation by increasing cell elongation and cell division (Davies, 1995; Fabian et al., 2000). In the GA-deficient *gal-3* background, all of the *spy* alleles increase stem elongation (up to one-third to one-fourth of wild type), by increasing cell length and the number of internodes (Silverstone et al., 1997; data not shown). However, in the presence of the *erecta* (*er*) mutation (in either the Col-0 or *Ler* background), the *spy-2* and *spy-4* mutants (in the wild-type

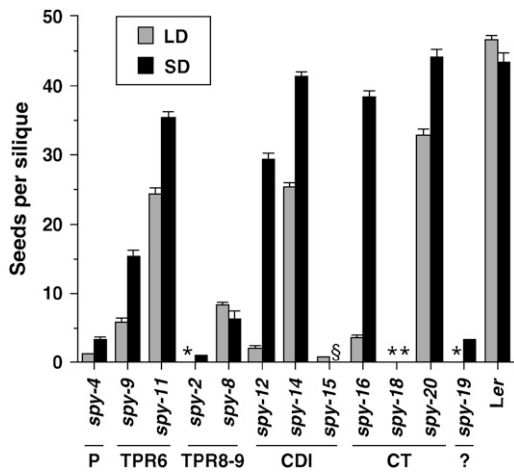


**Figure 3.** SD conditions partially restored the fertility of the *spy* mutants. Fertility was measured as the average number of seeds per silique in the first 15 siliques on the primary inflorescence stems of 10 plants that were grown in LD or SD conditions. The values plotted are the means  $\pm$  SE of 10 plants. The *spy* alleles are organized in the order of the mutations in the *SPY* genomic sequence. \*, Sterile; §, not determined.

*GA1* background) were reported to have significantly shorter internodes than wild type (Swain et al., 2001). This reduced internode length phenotype is likely due to an interaction between *er* and *spy* and may not be directly related to an alteration in GA response. The reduced fertility of *spy* mutants further complicate the effect of these alleles on stem height, because an increase in sterility leads to delayed cessation of proliferation of the inflorescence meristem and, hence, an increase in silique number and stem height (Hensel et al., 1994). We analyzed the final primary stem heights of the *spy* alleles to determine whether the tallest plants were the most sterile and produced the most siliques (Table II). This was the case for *spy-2* and *-18*, which were sterile and 22% to 28% taller than wild type in LD. Nevertheless, *spy-19*, which was also sterile in LD, was actually shorter than wild type, whereas in SD it is only 25% taller compared to wild type. By examining the average length of the internodes between siliques, it is possible to differentiate between growth of internodes and production of nodes. For all the *spy* alleles, there was a reduction of average internode length (height/node) and an increase in number of nodes. These results indicated that the effect of *spy* on stem height is complex and cannot be explained simply by an alteration of GA signaling.

### Trichomes

GA induces the expression of a MYB transcription factor, *GL1*, which is essential for trichome initiation (Perazza et al., 1998). The GA-deficient *gal-3* mutant has reduced adaxial trichomes and does not produce any abaxial trichomes (Chien and Sussex, 1996). GA also affects trichome morphogenesis. In *Arabidopsis*, 80% of trichomes on the rosette leaves of wild-type

plants (*Ler*) have three branches and 20% have four branches (Perazza et al., 1998). The *spy-5* allele was reported to cause a 2-fold increased production of the four branch trichomes (Perazza et al., 1998). Among the 12 *spy* alleles examined, we found that five additional *spy* alleles also exhibited an increase in trichome branching (Fig. 4A; data not shown). The effect of *spy-4*, *-16*, and *-20* is similar to *spy-5*, whereas *spy-2* and *spy-18* produced predominantly four branch trichomes (data not shown). The *spy-2* allele results in deletion of the TPR-8 and -9 motifs, and mutations in *spy-5*, *-16*, *-18*, and *-20* are all localized in the C-terminal coding region, suggesting that these regions are important for *SPY*'s function in regulating trichome development.

### Phyllotaxy

*Arabidopsis* normally produces plants with a spiral phyllotaxy for its flowers on the inflorescence stems. Previous studies indicated that the *spy-4* allele in the *Col-0* background showed altered inflorescence phyllotaxy (Swain et al., 2001). In the *Ler* background, *spy-2* and *spy-18*, in addition to *spy-4*, also exhibited this phenotype (Fig. 4B). The flowers of these alleles often initiated in a disordered fashion and sometimes with multiple flowers appearing to initiate from the same node. These observations indicated that TPR8, TPR9, and the C-terminal region of *SPY* are required for regulating the phyllotaxy of flowers on the inflorescence stem.

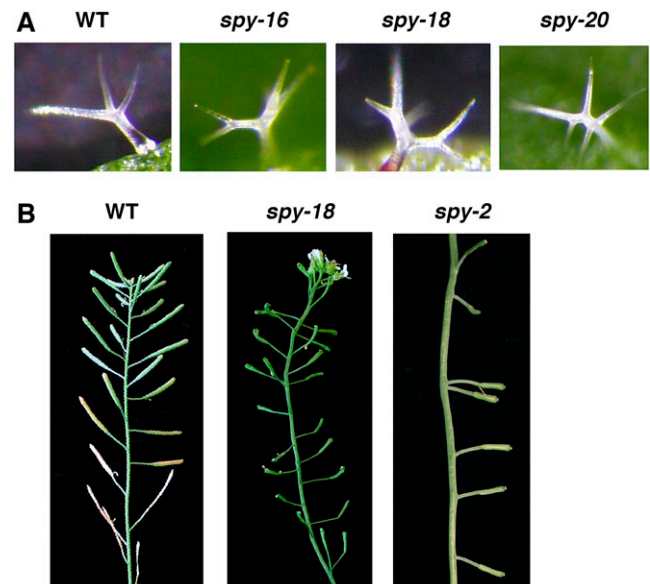


**Figure 4.** Abnormal trichome branching and inflorescence phyllotaxis in the *spy* mutants. A, Most of the trichomes on wild-type *Ler* leaves have three branches, whereas *spy-16*, *-18*, and *-20* produce higher percentages of four branched trichomes. Examples of three- (wild type), four- (*spy-16* and *-18*), and five-branch trichomes are shown. B, *spy-2* and *spy-18* showed abnormal inflorescence phyllotaxis in comparison to wild-type *Ler*. [See online article for color version of this figure.]

## Embryogenesis

Arabidopsis seedlings have two opposite cotyledons that are produced during embryogenesis. During the course of this work, it was noted that some *spy* alleles caused a partially penetrant defect in seedling cotyledon number. Therefore, several of the *spy* alleles were examined in more detail for this phenotype (Table III). The effect of *spy* in both Col-0 and *Ler* backgrounds was examined to determine if the phenotype exhibited any background dependence. To varying extents, the *spy* alleles examined increased the frequency of seedlings with one, two fused, or three cotyledons relative to the corresponding wild type. While no wild-type Col-0 or *gai-1* seedlings exhibited this phenotype, a proportion of *spy-1*, *-2*, *-3*, and *-4* seedlings had abnormal cotyledons, with the phenotype being most penetrant in *spy-2*. Cotyledon defects were also observed in *gai-1 spy-2* double mutants but were complemented by the addition of a genomic clone containing the entire *SPY* gene (data not shown). Although some abnormal cotyledons were observed in *Ler* plants, the frequency was higher when a *spy* allele was present.

*spy* Partially Suppresses the Dwarf Phenotype of *rga-Δ17*

The mechanism of the interaction between SPY and the DELLA proteins (RGA, GAI, and RGLs) in GA signaling is not clear, although genetic studies indicated that these proteins are all negative regulators of GA signaling. The loss-of-function *rga* and *spy-8* alleles have a synergistic effect in rescuing the dwarf phenotype of the GA-deficient mutant *gai-3* (Silverstone et al., 1997). Because *spy-8* is not a null allele, RGA and SPY may act in the same pathway or in two parallel pathways. Previous studies also showed that *spy* mutations suppress the dwarf phenotype of the gain-of-function *gai-1* allele (Wilson and Somerville, 1995; Jacobsen et al., 1996; Peng et al., 1997). To investigate further the relationship between RGA and SPY in GA signaling, we tested whether *spy* suppresses the gain-of-function *rga-Δ17* allele. When comparing phenotypes of the homozygous *rga-Δ17* line and the double homozygous *spy-8 rga-Δ17* plant (Fig. 5; Table IV), we found that *spy-8* partially rescued all the phenotypes of *rga-Δ17* but did not restore its GA responsiveness. These results are consistent with the hypothesis that SPY may activate the DELLA proteins by GlcNAc

**Table II.** Final stem height, silique number, and internode length of wild type and the *spy* alleles in LD and SD conditions

Values for height and silique number are means  $\pm$  SE.

<i>spy</i> Allele	Affected Region <sup>a</sup>	Height	Silique	Average Internode Length
		cm	n	mm
LD				
<i>spy-4</i>	P	14.3 $\pm$ 0.2	50.6 $\pm$ 1.7	2.8
<i>spy-9</i>	TPR6	15.4 $\pm$ 1.1	35.7 $\pm$ 1.9	4.3
<i>spy-11</i>	TPR6	11.7 $\pm$ 0.9	20.6 $\pm$ 2.1	5.7
<i>spy-2</i>	TPR8-9	25.8 $\pm$ 0.6	72.2 $\pm$ 2.3	3.6
<i>spy-8</i>	TPR8-9	22.0 $\pm$ 0.9	59.3 $\pm$ 3.0	3.7
<i>spy-12</i>	CDI	18.1 $\pm$ 0.7	41.8 $\pm$ 2.2	4.3
<i>spy-14</i>	CDI	14.2 $\pm$ 0.4	35.7 $\pm$ 1.7	4.0
<i>spy-15</i>	CDI	17.2 $\pm$ 1.1	34.6 $\pm$ 3.7	5.0
<i>spy-16</i>	CT	19.7 $\pm$ 0.7	53.8 $\pm$ 2.8	3.7
<i>spy-18</i>	CT	24.6 $\pm$ 2.0	64.5 $\pm$ 5.7	3.8
<i>spy-20</i>	CT	16.4 $\pm$ 0.5	30.0 $\pm$ 1.1	5.5
<i>spy-19</i>	?	17.6 $\pm$ 0.3	56.3 $\pm$ 3.2	3.1
<i>Ler</i>		20.2 $\pm$ 0.5	30.9 $\pm$ 1.1	6.5
SD				
<i>spy-4</i>	P	13.2 $\pm$ 1.1	66.8 $\pm$ 6.5	2.0
<i>spy-9</i>	TPR6	18.1 $\pm$ 0.8	59.9 $\pm$ 2.8	3.0
<i>spy-11</i>	TPR6	14.5 $\pm$ 0.8	68.1 $\pm$ 3.0	2.1
<i>spy-2</i>	TPR8-9	28.5 $\pm$ 1.7	129.9 $\pm$ 8.0	2.2
<i>spy-8</i>	TPR8-9	11.5 $\pm$ 0.7	65.7 $\pm$ 4.3	1.8
<i>spy-12</i>	CDI	15.9 $\pm$ 0.6	58.2 $\pm$ 3.0	2.7
<i>spy-14</i>	CDI	15.2 $\pm$ 0.6	47.6 $\pm$ 1.4	3.2
<i>spy-15</i>	CDI	n.d. <sup>b</sup>	n.d.	n.d.
<i>spy-16</i>	CT	23.6 $\pm$ 1.1	65.4 $\pm$ 3.0	3.6
<i>spy-18</i>	CT	32.7 $\pm$ 1.4	130.9 $\pm$ 5.7	2.5
<i>spy-20</i>	CT	17.9 $\pm$ 1.0	48.8 $\pm$ 2.2	3.7
<i>spy-19</i>	?	24.4 $\pm$ 1.1	74.0 $\pm$ 5.6	3.3
<i>Ler</i>		18.0 $\pm$ 0.5	41.2 $\pm$ 2.3	4.4

<sup>a</sup>The alleles are organized in the order of the mutations in the *SPY* genomic sequences. P, Promoter; CT, C terminus. <sup>b</sup>Not determined.

modification. In animal systems, GlcNAc modification can affect target proteins at multiple levels, including inhibition of phosphorylation, increased protein stability, altered nuclear localization, or protein activity (Wells et al., 2001). We therefore analyzed the effect of *spy-8* on the levels and localization of the RGA and/or *rga-Δ17* proteins. Unexpectedly, immunoblot analysis demonstrated that the *spy-8* mutation causes an increase (instead of a reduction) in the amount of RGA and *rga-Δ17* proteins (Fig. 6, A and B). The *spy-8* mutation did not affect GA-induced degradation of RGA (Fig. 6A), consistent with the previous observation that *spy* mutants remain GA responsive (Silverstone et al., 1997). Several additional *spy* alleles (*spy-9*, *-12*, *-13*, *-15*, and *-17*) also accumulate a higher amount of the RGA protein than wild type (Fig. 6C), indicating that this effect is not specific for the *spy-8* allele.

As shown previously (Dill et al., 2001), an extra faint protein band (form II) with a slower mobility than *rga-Δ17* (form I) is present in protein extracts from *rga-Δ17* plants (Fig. 6B). Both form I and form II of the *rga-Δ17* protein (Fig. 6B) accumulated to a higher level in the *spy-8* background, but the amount of form II increased more dramatically than form I. It is possible that the form II protein may be phosphorylated *rga-Δ17*, and, similar to *O*-GlcNAc modifications made by animal OGT, modification by SPY may block phosphorylation of RGA.

We also analyzed the impact of *spy* on the amounts of RGA and *rga-Δ17* transcript accumulation by quantitative real-time reverse transcription (RT)-PCR using gene-specific primers (Fig. 6D). The RGA mRNA level in *spy-8* is similar to wild type, indicating that the elevated amount of the RGA protein in *spy-8* is not caused by an increased RGA transcript level. The RNA for *rga-Δ17* was isolated from a mixed population of homozygous and hemizygous seedlings, because homozygous *rga-Δ17* is sterile, whereas RNA for *spy-8 rga-Δ17* was isolated from homozygous plants. Both

*rga-Δ17* and *spy-8 rga-Δ17* plants contain two copies of the wild-type RGA locus and one or two copies of the *rga-Δ17* transgene, and the amounts of the RGA transcript measured are the combination of both RGA and *rga-Δ17* mRNAs. *rga-Δ17* accumulates a wild-type level of the RGA mRNA, whereas *spy-8 rga-Δ17* contains 2-fold higher amount of the RGA transcript. The slightly increased RGA mRNA level in *spy-8 rga-Δ17* could be due to the extra copy of the *rga-Δ17* transgene and/or altered feedback regulation of RGA expression resulting from the elevated activity in the GA response pathway that is caused by the *spy* mutation.

To examine the effect of *spy* on the subcellular localization of RGA, we generated a *spy-8* line that contains the *PRGA:green fluorescent protein (GFP)-RGA* transgene by crosses between *spy-8* and a previously characterized transgenic *Ler/PRGA:GFP-RGA* line (Silverstone et al., 2001). This *PRGA:GFP-RGA* fusion gene was able to rescue the phenotype of a null *rga* allele, and the GFP-RGA fusion is localized to the nucleus in transgenic Arabidopsis (Silverstone et al., 2001; Fig. 6E). Confocal microscopy showed that loss of the SPY function does not alter the nuclear localization of the GFP-RGA protein in *spy-8 GFP-RGA*. Thus, SPY may modify and convert the RGA protein to a more active form, which may be tightly regulated by controlled proteolysis. In contrast, the less active form of RGA and *rga-Δ17* in the *spy-8* background may accumulate to a higher level.

## DISCUSSION

To date, 20 loss-of-function *spy* alleles with defects in GA signaling have been identified (Fig. 1; Table I). The molecular defects of 19 of them have been characterized, and all of them except *spy-4* contain mutations that are localized either in three of the TPRs (TPR6, TPR8, and TPR9) or in the catalytic C-terminal region

**Table III.** Several *spy* alleles increase the frequency of seedlings with abnormal cotyledons

Genotype	Background	Total Seed No. <sup>a</sup>	Abnormal Seedlings	% Abnormal Seedlings
Wild type	Col-0	850	0	0.00
<i>spy-1 hy-2</i>	Col-0	760	27	3.55
<i>spy-2</i>	Col-0	456	21	4.61
<i>spy-3</i>	Col-0	1,849	7	0.38
<i>spy-4</i>	Col-0 (BC6) <sup>b</sup>	598	4	0.67
<i>gai-1</i>	Col-0 (BC3)	291	0	0.00
Wild type	Ler	904	2	0.22
<i>spy-2</i>	Ler (BC3)	163	16	9.82
<i>spy-4</i>	Ler (BC3)	227	1	0.44
<i>spy-5</i>	Ler	986	5	0.71
<i>spy-18</i>	Ler	405	52	12.83
<i>spy-19</i>	Ler	127	15	11.84

<sup>a</sup>For *spy-2* (Col-0 and Ler), *spy-4* (Ler), *spy-18*, and *spy-19*, a segregating population was analyzed, and the number of seeds examined represents 25% of the seeds analyzed from heterozygous *SPY spy* parents. The number reported for the other genotypes is the actual number of homozygous seeds analyzed.

<sup>b</sup>The backcross (BC) generation into this background is indicated.

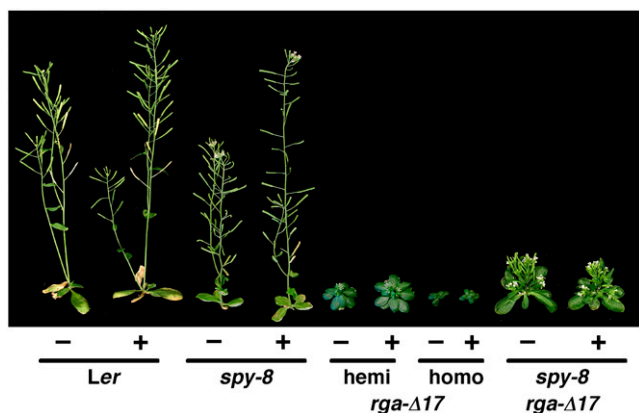


**Figure 5.** *spy-8* partially suppresses *rga-Δ17* but does not restore GA responsiveness. Plants were grown on soil for 36 d with 100  $\mu\text{M}$  GA<sub>3</sub> (+) or water (-) treatment (starting at day 18). All plants are homozygous for the genotype(s) indicated, except *rga-Δ17*; homo, plants are homozygous for *rga-Δ17*; hemi, plants are hemizygous for *rga-Δ17*. Representative plants are shown. The inflorescence stems of the *spy-8* plants grew slower than wild type, but the final height is similar to wild type (Table II). [See online article for color version of this figure.]

of the OGT domain in SPY (Fig. 1). Phenotypic characterization of 12 *spy* alleles revealed that mutations in TPRs 6, 8, and 9 or the catalytic region affect GA signaling in floral induction and fertility. These sequences in SPY are also important for repressing GA-induced stem elongation, because all *spy* alleles partially suppress the dwarf phenotype of the GA-deficient mutant *ga1*, even though the *spy* single mutants are not always taller than wild-type *Ler*. Our results suggest that SPY regulates GA signaling through specific protein-protein interactions via TPRs 6, 8, and 9, and its OGT catalytic activity. The other TPRs may be important for SPY to function in other cellular pathways. We cannot rule out the possibility that the currently available *spy* alleles may affect SPY protein stability in general. Alternatively, the clustered mutations in these alleles may reflect the hot spots of mutagenesis, although they were generated by ethyl

methanesulfonate (EMS),  $\gamma$ -radiation, or fast neutron (Table I).

### The TPRs and the Catalytic Region Are Important for SPY's Function in GA Signaling

Six of the newly characterized *spy* mutations affect the TPR domain, and these, together with the previously characterized *spy-1* and *spy-2* mutations (Jacobsen et al., 1996), are clustered in TPRs 6, 8, and/or 9 (Fig. 1A). Four alleles represent missense mutations affecting Gly-268 of TPR 6. The *spy-7* mutation deletes part of TPR9 and also changes an amino acid. *spy-8* has the same mutation as *spy-1*; the last G of exon 8 is mutated to an A. The *spy-1* mutation has been shown to cause an error in splicing that results in exon 8 being skipped. Interestingly, *spy-2* affects the last G of intron 7 and also causes exon 8 to be skipped. The deletion of exon 8 from the SPY mRNA causes the in-frame deletion of portions of TPRs 8 and 9 from the SPY protein. While *spy-2* has more severe phenotypes than *spy-1* (data not shown) and *spy-8*, RT-PCR analysis indicates that in *spy-1*, but not *spy-2*, a small amount of wild-type-sized transcript is produced (S.E. Jacobsen and N.E. Olszewski, unpublished data). Therefore, *spy-1* and *spy-8* are probably weaker alleles than *spy-2*, because they encode a small amount of wild-type transcript. The clustering of mutations in TPRs 6, 8, and 9 suggested that only these TPRs are essential for GA signaling or that mutations affecting the other TPRs cause different phenotypes.

Gly-268, which is mutated to Glu in *spy-6*, *spy-10*, and *spy-11*, and to Arg in *spy-9*, is located at the position 8 in TPR 6 (Fig. 1B). A Gly residue is present at position 8 of all 10 SPY TPRs (Jacobsen et al., 1996). The amino acid residue at position 8 of TPRs is generally small and hydrophobic (Das et al., 1998; Blatch and Lässle, 1999). In the TPR crystal structure (Das et al., 1998; Scheufler et al., 2000; Jinek et al., 2004), position 8 is at the closest contact between a pair of antiparallel  $\alpha$  helices, and a bulky residue at this position is predicted to affect the positioning of these helices (Das

**Table IV.** *spy-8* partially suppresses all phenotypes of *rga-Δ17*

Values are means  $\pm$  SE. hemi, Hemizygous; homo, homozygous; n.d., not determined. Final height for *rga-Δ17* homozygotes was not determined, because they did not bolt. Branch number for *rga-Δ17* homozygotes was not determined, because they died shortly after flowering.

Genotype	Flowering Time		Final Height	Rosette Diameter	Branch No.	Seeds/Silique	
	Total Leaves <sup>a</sup>	Days				All <sup>b</sup>	Fertile <sup>c</sup>
<i>Ler</i>	6.9 $\pm$ 0.2	14.9 $\pm$ 0.5	15.1 $\pm$ 0.4	18.3 $\pm$ 0.5	3.0 $\pm$ 0.2	36.5 $\pm$ 1.2	36.5 $\pm$ 1.2
<i>spy-8</i>	5.4 $\pm$ 0.3	13.8 $\pm$ 0.3	16.5 $\pm$ 1.6	7.4 $\pm$ 0.3	2.8 $\pm$ 0.3	2.7 $\pm$ 0.3	4.8 $\pm$ 0.4
<i>rga-Δ17</i> hemi	13.4 $\pm$ 0.5	23.5 $\pm$ 0.7	3.6 $\pm$ 0.2	19.6 $\pm$ 0.5	10.8 $\pm$ 0.6	3.4 $\pm$ 0.4	15.1 $\pm$ 1.0
<i>rga-Δ17</i> homo	14.0 $\pm$ 0.9	26.9 $\pm$ 1.2	No bolting	9.0 $\pm$ 0.4	n.d.	Sterile	Sterile
<i>spy-8 rga-Δ17</i>	8.5 $\pm$ 0.3	16.3 $\pm$ 0.5	2.7 $\pm$ 0.2	18.2 $\pm$ 0.5	6.0 $\pm$ 0.4	26.0 $\pm$ 0.8	26.0 $\pm$ 0.8

<sup>a</sup>Total leaves includes rosette and cauline leaves. <sup>b</sup>Fertility was measured by the number of seeds per silique on the primary inflorescence stem for 10 plants per line. The number of seeds in all siliques were counted and then averaged. <sup>c</sup>As in b, except that seeds per silique were averaged using only siliques that contained at least one seed. *spy-8* and *rga-Δ17* hemizygotes contain many completely sterile siliques.

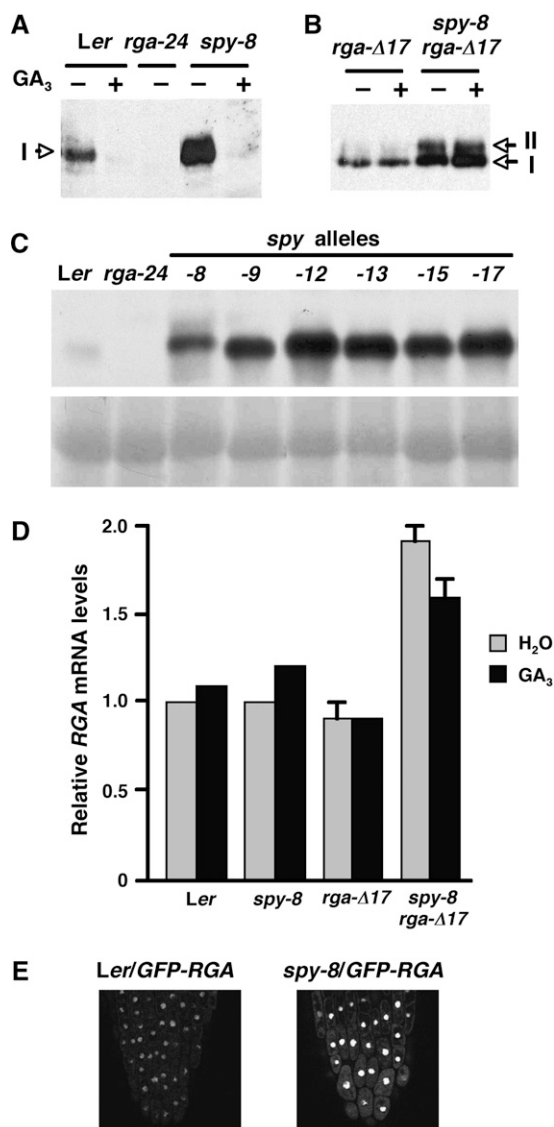


**Figure 6.** The levels of RGA and *rga-Δ17* proteins, but not mRNA, are elevated in the *spy* mutant backgrounds. A to C, The blots contain 25  $\mu\text{g}$  (in A and B) or 50  $\mu\text{g}$  (in C) total protein from 8-d-old seedlings after 2-h treatment with water (–) or 100  $\mu\text{M}$   $\text{GA}_3$  (+) as labeled. Affinity-purified rabbit anti-RGA antibodies were used to detect the RGA (64 kD) and *rga-Δ17* (62 kD) proteins (form I). The extra band (form II) may be a modified *rga-Δ17*. The images in B were developed after a shorter exposure on film than A and C. An image of the Ponceau-stained blot is shown below the immunoblot in C to confirm equal loading. D, Relative RGA mRNA levels determined by quantitative RT-PCR. Total RNA was isolated from wild type and various mutants after 100  $\mu\text{M}$   $\text{GA}_3$  (+) or water (–) treatment for 2 h. The relative RGA mRNA levels were determined by running three quantitative RT-PCR reactions for each sample and normalized using the housekeeping gene *GAPC*. Bars = means  $\pm$  SE. The value of water-treated wild type was arbitrarily set to 1.0. Proteins or mRNA in A to D were extracted from homozygous lines as labeled, except that the sample for the *rga-Δ17* line was extracted from a mixture of hemi- and homozygous plants. E, GFP fluorescence in root tips of transgenic lines expressing GFP-RGA in wild-type or *spy-8* backgrounds. The images were captured by confocal laser microscopy under an identical setting.

et al., 1998; Gounalaki et al., 2000; Scheufler et al., 2000). Mutations affecting position 8 disrupt the interaction with other proteins (de Boer et al., 1994; Ponting, 1996; Gounalaki et al., 2000). Therefore, the mutations affecting Gly-268 may be disrupting interactions between the enzyme subunits, interactions with a substrate, and/or interaction with a protein that regulates SPY activity.

Ten of the *spy* alleles are mutated in the C terminus of SPY, which is likely to be the catalytic domain. OGT catalytic domains contain two conserved regions, designated CDI and II, that are predicted to contribute to the formation of a UDP-GlcNAc-binding pocket that participates in transferring the sugar to the substrate (Lazarus et al., 2005). CDI is affected in *spy-3*, *spy-12*, *spy-13*, *spy-14*, and *spy-15*, while *spy-5*, *spy-16*, *spy-17*, *spy-18*, and *spy-20* all are mutated near CDII (Figs. 1, A and C).

#### TPR8, TPR9, and the C Terminus of SPY Are Important for Regulating Trichome Branching and Inflorescence Phyllotaxy

Our studies suggested that TPRs 8 and 9 (partially deleted in *spy-2*) and the C-terminal region (deleted in *spy-18*) also play an essential role in regulating trichome development and inflorescence phyllotaxy. GA is important for trichome initiation (Chien and Sussex, 1996) and branching (Perazza et al., 1998). We found that *spy* alleles that affect TPRs 8 and 9 or the C terminus produced higher percentages of four-branch trichomes than wild type. Previously genetic studies revealed that mutations in four additional genes *POLYCHOME* (*PYM*), *KAKTUS* (*KAK*), *RASTAFARI* (*RFI*), and *TRIPTYCHOME* (*TRY*) also result in over-branched trichome development (Perazza et al., 1999). However, unlike the *spy* mutants, none of these mutants exhibit GA-related phenotypes in seed germination or floral induction. Epistasis analysis demonstrated that *PYM*, *KAK*, and *RFI* are likely to be downstream of SPY in the same pathway, whereas *TRY* is located in a separate pathway from SPY (Perazza et al., 1999). These findings suggest that SPY may affect trichome development through a branch of the GA signaling pathway.

Changes in leaf phyllotaxis have been observed in GA-treated *Xanthium pennsylvanicum* (Maksymowych and Erickson, 1977). However, in *Arabidopsis*, GA-deficient mutants and most of the GA-response mutants (except *spy*) do not exhibit aberrant phyllotaxis, suggesting that SPY may modulate phyllotaxis by interacting with components in another cellular pathway. It remains to be determined whether GA plays a role in regulating phyllotaxis in most species. Recent studies indicate that polar transport of auxin is involved in regulating the initiation and radial position of lateral organs in the *Arabidopsis* inflorescence meristem (Reinhardt et al., 2000, 2003). Cytokinin may also regulate phyllotaxis by inducing expansion of the shoot meristem, as suggested by the characterization

of an altered phyllotaxy maize (*Zea mays*) mutant *abph1* that is defective in a putative negative cytokinin response regulator (Giulini et al., 2004). Future analysis will be needed to determine whether SPY affects phyllotaxy by interacting with components in the cytokinin and/or auxin pathway.

### SPY Has a Role in Embryo Development

Mutations in either the TPR domain or the catalytic domain caused a partially penetrant defect in cotyledon development (Table III). The primary defect in these mutants appears to be in the positioning and initiation of the cotyledons during embryogenesis. This is supported by the observations that mutant seedlings could have one, two fused, or three cotyledons. SPY has previously been shown to have a role in embryogenesis, because *sec spy* double mutant embryos fail to complete development (Hartweck et al., 2002). It is not clear whether the cotyledon phenotype in the *spy* mutants is due to altered GA signaling or defects in other developmental pathways, but GAs have been suggested to be essential for Arabidopsis seed development (Singh et al., 2002).

### SPY Is Not Required for Nuclear Localization or Increased Stability of RGA

Based on the functions of animal OGTs, we previously hypothesized that SPY may activate RGA by GlcNAc modification (Silverstone et al., 1998). This idea is supported by a recent finding that the paralog of SPY, SEC, GlcNAc modifies RGA in a heterologous system (L. Hartweck and N.E. Olszewski, unpublished data). Here, we showed that GFP-RGA fusion protein is still localized to the nucleus in the *spy* mutant background. We further demonstrated that the *spy* mutation does not destabilize the RGA protein. These results eliminated the possibility that the nuclear localization and stability of RGA depend on SPY function. We therefore propose that the role of SPY is to directly increase RGA protein activity via O-GlcNAcylation. In *rga-Δ17* plants, an extra protein band (form II) with a slower mobility than *rga-Δ17* (form I) is present (Dill et al., 2001; Fig. 6B). Similarly, the gain-of-function DELLA mutant protein (*sln1-d*) in barley is also present in two forms (Gubler et al., 2002). The *spy* mutation caused an increased accumulation of both form I and form II of the *rga-Δ17* protein, although the amount of form II appeared to increase more dramatically (Fig. 6B). This form II protein may be *rga-Δ17* with posttranslational modification(s), although the nature of the modification has not been identified. One possibility is that form II may be phosphorylated *rga-Δ17*, and, similar to animal OGT, SPY may prevent phosphorylation of RGA. However, the form II of *rga-Δ17* and *sln1-d* remains stable after GA treatment (Fig. 6B; Gubler et al., 2002), indicating that this specific modification is not sufficient to target these proteins for GA-induced degradation. This would be consistent

with the results of two recent studies (although mutually conflicting); one shows that phosphorylation of the rice DELLA protein SLR1 is independent of its degradation in response to GA (Itoh et al., 2005), whereas the other suggests that dephosphorylation of RGL2 is required for its degradation (Hussain et al., 2005). Our model is mainly based on genetic data and on the effect of *spy* on RGA localization and stability. Alternatively, SPY and RGA may function independently in GA signaling. Additional biochemical studies are necessary to elucidate the nature of posttranslational modification in RGA and to investigate whether RGA is a substrate of SPY and whether GlcNAc modification of RGA increases RGA's activity in transcriptional regulation.

## MATERIALS AND METHODS

### Plant Lines and Mutant Phenotype Characterization

The original *spy-2* and *spy-4* mutants were isolated in the Col-0 and Wassilewskija ecotype backgrounds, respectively (Jacobsen and Olszewski, 1993; Jacobsen et al., 1996). To minimize the effect of different ecotype backgrounds, homozygous *spy-2* and *spy-4* lines that had been crossed with *Ler* (three times for *spy-2* and four times for *spy-4*) were used in this study. The *spy-6* (EMS) and *spy-7* ( $\gamma$ -radiation; previously named *gas1-1*) alleles were obtained from S.E. Jacobsen and N. Harberd (Peng et al., 1997), respectively. *spy-8* to *spy-17* (EMS) and *spy-18* to *spy-20* (fast neutron) were obtained from screening suppressor mutations that rescued the *ga1-3* phenotype (Silverstone et al., 1997, 1998). The double homozygous *spy ga1-3* plants were crossed with *Ler* plants, and the *spy* single mutants were identified in the F<sub>2</sub> generation by their *spy* phenotype. The *spy-18* and *spy-19* alleles were maintained as heterozygous lines, because the homozygotes in LD conditions are sterile. The *spy-8 rga-Δ17* double mutant was generated by genetic crosses between *spy-8* and a transgenic *Ler* line that carries the *PRGA:rga-Δ17* fusion gene (Dill et al., 2001). The double homozygous *spy-8 rga-Δ17* plants were selected using the kanamycin-resistant marker (linked to the transgene) and by PCR using allele-specific cleaved amplified polymorphic sequence (CAPS) primers for *spy-8* and *SPY*. Amplification of *SPY* and *spy-8* genomic DNA using primer 400 (5'-AGGCTTGCAACAATTGGGAG-3') and primer 401 (5'-CCTTCTCAATCATGCTGGCA-3') will generate a 344-bp product. *ScrF1* digestion of the *spy-8* PCR DNA will produce 220- and 124-bp fragments, whereas *SPY* DNA remains 344 bp. For complementation of the cotyledon defect, the *gai-1 spy-2* 2118 genotype was made by crossing *gai-1 spy-2* (essentially in the Col-0 background; Swain et al., 2001) with No-0 plants containing a genomic *SPY* clone (2118) originally used for complementation studies (Jacobsen et al., 1996). Plants homozygous for *gai-1* and *spy-2* but hemizygous for the 2118 clone were identified and allowed to self pollinate. From these progeny plants homozygous for *gai-1* and *spy-2* without 2118 and plants homozygous for *gai-1*, *spy-2*, and 2118 were selected and progeny seed used for analyzing defects in cotyledon development.

For phenotypic characterization, the plants were grown under LD (16 h 140  $\mu$ E light/8 h dark) and/or SD (8 h 160  $\mu$ E light/16 h dark) conditions at 22°C. Ten plants of each line were used for the phenotypic measurements. The final height of the primary inflorescence stem of each plant was measured. The flowering time was scored as days to flower (when the flower bud was first visible without magnification) and as total number of leaves on the main stem. Fertility (average no. of seeds per silique) was measured by scoring the number of seeds in the first 15 siliques on the primary inflorescence stems of 10 plants.

### Mapping Mutations by Detection of SSCP

*spy* plants, together with wild-type Col-0 and *Ler*, were grown in continuous light at 23°C for 3 weeks. Leaves were prepared for PCR as described by Klimyuk et al. (1993), and the SSCP analysis was performed as described previously (Sheffield et al., 1993; Bailey, 1995). Primers for SSCP are listed in Supplemental Table S1.

## DNA Sequencing

DNA fragments with a SSCP between the wild-type and *spy* alleles were amplified by PCR from the alkaline-treated tissues in a 50- $\mu$ L volume of amplification solution containing 250  $\mu$ M of dNTPs (Pharmacia) without isotopes, 0.25  $\mu$ M of each of the two primers, in 1 $\times$  amplification buffer of 10 mM Tris-HCl, pH 8.3, 50 mM KCl, 2.5 mM MgCl<sub>2</sub>. Cycling conditions were: 94°C for 15 s; 52°C for 15 s; 72°C for 1 min; 35 cycles, followed by a 10-min extension at 72°C. PCR primers are listed in Supplemental Table S1. Amplified DNA fragments were gel purified for sequencing using the *fmol* sequencing kit (Promega) according to manufacturer's instructions.

## Immunoblot Analysis of RGA and *rga- $\Delta$ 17* Proteins

Eight-day-old seedlings that were grown on Murashige and Skoog plates were treated with water or 100  $\mu$ M GA<sub>3</sub> for 2 h as described previously (Dill et al., 2004). The seeds of the *rga- $\Delta$ 17* line were produced from hemizygous parents, because homozygous plants are sterile. Wild-type seedlings were discarded, and a mixture of hemizygous and homozygous *rga- $\Delta$ 17* seedlings were treated and harvested for protein extraction. Total plant proteins were isolated and analyzed by immunoblot analysis using affinity-purified anti-RGA antibodies from a rabbit (DU176) as described (Silverstone et al., 2001). Ponceau staining was used to confirm equal loading.

## Analysis of RGA mRNA Levels by Quantitative RT-PCR

Thirteen-day-old seedlings that were grown on Murashige and Skoog agar plates were treated with water or 100  $\mu$ M GA<sub>3</sub> for 2 h as described previously (Dill et al., 2004). For *rga- $\Delta$ 17*, a mixture of hemizygous and homozygous *rga- $\Delta$ 17* seedlings were treated and harvested for RNA extraction (for the same reason described in the immunoblot analysis section). Total RNA was isolated, and the levels of RGA transcripts were quantified by real-time RT-PCR using gene-specific primers and a Roche Light Cycler as described (Dill et al., 2004). The housekeeping gene *GAPC* was used as a control to normalize all samples.

## Confocal Laser Microscopy

The *spy-8 GFP-RGA* line was generated by genetic crosses between *spy-8* and a transgenic *Ler* line that carries *PRGA:GFP-RGA* (Silverstone et al., 2001). The double homozygous *spy-8 GFP-RGA* plants were selected using the kanamycin-resistant marker (linked to the transgene) and by PCR using allele-specific primers for *spy-8* and *SPY* (see above). The root tips of 8-d-old *Ler GFP-RGA* and *spy-8 GFP-RGA* seedlings were excised with razor blades, and GFP fluorescence was detected by using a Zeiss LSM-410 confocal laser microscope as described (Silverstone et al., 2001).

## Supplemental Data

The following materials are available in the online version of this article.

**Supplemental Table S1.** Pairs of primers used for SSCP assays and DNA sequencing.

## ACKNOWLEDGMENTS

We thank N. Harberd for the *spy-7* seed and S. Jacobsen for the *spy-6* seed. We also thank Hou-Sung Jung for help with the generation of *spy-8 GFP-RGA* and confocal analysis and Lynn Hartweck for comments on the manuscript.

Received October 6, 2006; accepted November 23, 2006; published December 1, 2006.

## LITERATURE CITED

- Bailey AL (1995) Single-stranded conformational polymorphisms. In MA Innis, DH Gelfand, JJ Sninsky, eds, PCR Strategies. Academic Press, San Diego, pp 121–129
- Blatch GL, Lässle M (1999) The tetratricopeptide repeat: a structural motif mediating protein-protein interactions. *Bioessays* **21**: 932–939

- Carol P, Peng J, Harberd NP (1995) Isolation and preliminary characterization of *gas1-1*, a mutation causing partial suppression of the phenotype conferred by the gibberellin-insensitive (*gai*) mutation in *Arabidopsis thaliana* (L.) Heynh. *Planta* **197**: 414–417
- Cheng H, Qin L, Lee S, Fu X, Richards DE, Cao D, Luo D, Harberd NP, Peng J (2004) Gibberellin regulates *Arabidopsis* floral development via suppression of DELLA protein function. *Development* **131**: 1055–1064
- Chien JC, Sussex IM (1996) Differential regulation of trichome formation on the adaxial and abaxial leaf surfaces by gibberellins and photoperiod in *Arabidopsis thaliana* (L.) Heynh. *Plant Physiol* **111**: 1321–1328
- Comer FI, Hart GW (2001) Reciprocity between O-GlcNAc and O-phosphate on the carboxyl terminal domain of RNA polymerase II. *Biochemistry* **40**: 7845–7852
- Das AK, Cohen PTW, Barford D (1998) The structure of the tetratricopeptide repeats of protein phosphatase 5: implications for TPR-mediated protein-protein interactions. *EMBO J* **17**: 1192–1199
- Davies PJ, editor (1995) *Plant Hormones: Physiology, Biochemistry and Molecular Biology*. Kluwer Academic Publishers, Dordrecht, The Netherlands
- de Boer M, Hilarius-Stokman PM, Hossle JP, Verhoeven AJ, Graf N, Kenney RT, Seger R, Roos D (1994) Autosomal recessive chronic granulomatous disease with absence of the 67-kD cytosolic NADPH oxidase component: identification of mutation and detection of carriers. *Blood* **83**: 531–536
- Dill A, Jung H-S, Sun T-p (2001) The DELLA motif is essential for gibberellin-induced degradation of RGA. *Proc Natl Acad Sci USA* **98**: 14162–14167
- Dill A, Sun T-p (2001) Synergistic de-repression of gibberellin signaling by removing RGA and GAI function in *Arabidopsis thaliana*. *Genetics* **159**: 777–785
- Dill A, Thomas SG, Hu J, Steber CM, Sun T-p (2004) The *Arabidopsis* F-box protein SLEEPY1 targets GA signaling repressors for GA-induced degradation. *Plant Cell* **16**: 1392–1405
- Fabian T, Lorbiecke R, Umeda M, Sauter M (2000) The cell cycle genes *cycA1;1* and *cdc2Os-3* are coordinately regulated by gibberellin in planta. *Planta* **211**: 376–383
- Filardo F (2004) SPY, a negative regulator of GA response in *Arabidopsis thaliana*. An investigation of the TPR domain. PhD thesis. La Trobe University, Melbourne, Australia
- Fleet CM, Sun TP (2005) A DELLAcate balance: the role of gibberellin in plant morphogenesis. *Curr Opin Plant Biol* **8**: 77–85
- Fu X, Richards DE, Ait-ali T, Hynes LW, Ougham H, Peng J, Harberd NP (2002) Gibberellin-mediated proteasome-dependent degradation of the barley DELLA protein SLN1 repressor. *Plant Cell* **14**: 3191–3200
- Fu X, Richards DE, Fleck B, Xie D, Burton N, Harberd NP (2004) The *Arabidopsis* mutant *sleepy1<sup>gar2-1</sup>* protein promotes plant growth by increasing the affinity of the SCF<sup>SLEEPY1</sup> E3 ubiquitin ligase for DELLA protein substrates. *Plant Cell* **16**: 1406–1418
- Giulini A, Wang J, Jackson D (2004) Control of phyllotaxy by the cytokinin-inducible response regulator homologue ABPHYL1. *Nature* **430**: 1031–1034
- Gounalaki N, Tzamaras D, Vlasi M (2000) Identification of residues in the TPR domain of Ssn6 responsible for interaction with the Tup1 protein. *FEBS Lett* **473**: 37–41
- Greenboim-Wainberg Y, Maymon I, Borochoy R, Alvarez J, Olszewski N, Ori N, Eshed Y, Weiss D (2005) Cross talk between gibberellin and cytokinin: the *Arabidopsis* GA response inhibitor SPINDLY plays a positive role in cytokinin signaling. *Plant Cell* **17**: 92–102
- Gubler F, Chandler P, White R, Llewellyn D, Jacobsen J (2002) GA signaling in barley aleurone cells: control of SLN1 and GAMYB expression. *Plant Physiol* **129**: 191–200
- Hanover JA, Forsythe ME, Hennessey PT, Brodigan TM, Love DC, Ashwell G, Krause M (2005) A *Caenorhabditis elegans* model of insulin resistance: altered macronutrient storage and dauer formation in an OGT-1 knockout. *Proc Natl Acad Sci USA* **102**: 11266–11271
- Hartweck LM, Scott CL, Olszewski NE (2002) Two O-linked N-acetylglucosamine transferase genes of *Arabidopsis thaliana* L. Heynh. have overlapping functions necessary for gamete and seed development. *Genetics* **161**: 1279–1291
- Hayashi K (1992) PCR-SSCP: a method for detection of mutations. *Genet Anal Tech Appl* **9**: 73–79

- Hensell LL, Nelson MA, Richmond TA, Bleecker AB (1994) The fate of inflorescence meristems is controlled by developing fruits in Arabidopsis. *Plant Physiol* **106**: 863–876
- Hussain A, Cao D, Cheng H, Wen Z, Peng J (2005) Identification of the conserved serine/threonine residues important for gibberellin-sensitivity of Arabidopsis RGL2 protein. *Plant J* **44**: 88–99
- Itoh H, Sasaki A, Ueguchi-Tanaka M, Ishiyama K, Kobayashi M, Hasegawa Y, Minami E, Ashikari M, Matsuoka M (2005) Dissection of the phosphorylation of rice DELLA protein, SLENDER RICE1. *Plant Cell Physiol* **46**: 1392–1399
- Itoh H, Ueguchi-Tanaka M, Sato Y, Ashikari M, Matsuoka M (2002) The gibberellin signaling pathway is regulated by the appearance and disappearance of SLENDER RICE1 in nuclei. *Plant Cell* **14**: 57–70
- Jacobsen SE, Binkowski KA, Olszewski NE (1996) SPINDLY, a tetratricopeptide repeat protein involved in gibberellin signal transduction in Arabidopsis. *Proc Natl Acad Sci USA* **93**: 9292–9296
- Jacobsen SE, Olszewski NE (1993) Mutations at the SPINDLY locus of Arabidopsis alter gibberellin signal transduction. *Plant Cell* **5**: 887–896
- Jinek M, Rehwinkel J, Lazarus BD, Izaurralde E, Hanover JA, Conti E (2004) The superhelical TPR-repeat domain of O-linked GlcNAc transferase exhibits structural similarities to importin alpha. *Nat Struct Mol Biol* **11**: 1001–1007
- King K, Moritz T, Harberd N (2001) Gibberellins are not required for normal stem growth in Arabidopsis thaliana in the absence of GAI and RGA. *Genetics* **159**: 767–776
- Klimyuk VI, Carroll BJ, Thomas CM, Jones JD (1993) Alkali treatment for rapid preparation of plant material for reliable PCR analysis. *Plant J* **3**: 493–494
- Koornneef M, van der Veen JH (1980) Induction and analysis of gibberellin-sensitive mutants in Arabidopsis thaliana (L.) Heynh. *Theor Appl Genet* **58**: 257–263
- Kreppel L, Blomberg MA, Hart GW (1997) Dynamic glycosylation of nuclear and cytosolic proteins. *J Biol Chem* **272**: 9308–9315
- Kreppel LK, Hart GW (1999) Regulation of a cytosolic and nuclear O-GlcNAc transferase: role of the tetratricopeptide repeats. *J Biol Chem* **274**: 32015–32022
- Lazarus BD, Roos MD, Hanover JA (2005) Mutational analysis of the catalytic domain of O-linked N-acetylglucosaminyl transferase. *J Biol Chem* **280**: 35537–35544
- Lee S, Cheng H, King KE, Wang W, He Y, Hussain A, Lo J, Harberd NP, Peng J (2002) Gibberellin regulates Arabidopsis seed germination via RGL2, a GAI/RGA-like gene whose expression is up-regulated following imbibition. *Genes Dev* **16**: 646–658
- Love DC, Hanover JA (2005) The hexosamine signaling pathway: deciphering the “O-GlcNAc code”. *Sci STKE* **2005**: re13
- Lubas WA, Frank DW, Krause M, Hanover JA (1997) O-linked GlcNAc transferase is a conserved nucleocytoplasmic protein containing tetratricopeptide repeats. *J Biol Chem* **272**: 9316–9324
- Lubas WA, Hanover JA (2000) Functional expression of O-linked GlcNAc transferase: domain structure and substrate specificity. *J Biol Chem* **275**: 10983–10988
- Maksymowycz R, Erickson RO (1977) Phylloclastic change induced by gibberellic acid in Xanthium shoot spines. *Am J Bot* **64**: 33–44
- McGinnis KM, Thomas SG, Soule JD, Strader LC, Zale JM, Sun T-p, Steber CM (2003) The Arabidopsis SLEEPY1 gene encodes a putative F-box subunit of an SCF E3 ubiquitin ligase. *Plant Cell* **15**: 1120–1130
- Moir RD, Sethy-Coraci I, Puglia K, Librizzi MD, Willis IM (1997) A tetratricopeptide repeat mutation in yeast transcription factor IIIC131 (TFIIIC131) facilitates recruitment of TFIIIB-related factor TFIIIB70. *Mol Cell Biol* **17**: 7119–7125
- Nakajima M, Shimada A, Takashi Y, Kim YC, Park SH, Ueguchi-Tanaka M, Suzuki H, Katoh E, Iuchi S, Kobayashi M, et al (2006) Identification and characterization of Arabidopsis gibberellin receptors. *Plant J* **46**: 880–889
- Ollendorff V, Donoghue DJ (1997) The serine/threonine phosphatase PP5 interacts with CDC16 and CDC27, two tetratricopeptide repeat-containing subunits of the anaphase-promoting complex. *J Biol Chem* **272**: 32011–32018
- Olszewski N, Sun T-p, Gubler F (2002) Gibberellin signaling: biosynthesis, catabolism, and response pathways. *Plant Cell (Suppl)* **14**: S61–S80
- Peng J, Carol P, Richards DE, King KE, Cowling RJ, Murphy GP, Harberd NP (1997) The Arabidopsis GAI gene defines a signalling pathway that negatively regulates gibberellin responses. *Genes Dev* **11**: 3194–3205
- Peng J, Harberd NP (2002) The role of GA-mediated signalling in the control of seed germination. *Curr Opin Plant Biol* **5**: 376–381
- Perazza D, Herzog M, Hulskamp M, Brown S, Dorne AM, Bonneville JM (1999) Trichome cell growth in Arabidopsis thaliana can be derepressed by mutations in at least five genes. *Genetics* **152**: 461–476
- Perazza D, Vachon G, Herzog M (1998) Gibberellins promote trichome formation by up-regulating GLABROUS1 in Arabidopsis. *Plant Physiol* **117**: 375–383
- Ponting CP (1996) Novel domains in NADPH oxidase subunits, sorting nexins, and PtdIns 3-kinases: binding partners of SH3 domains? *Protein Sci* **5**: 2353–2357
- Reinhardt D, Mandel T, Kuhlemeier C (2000) Auxin regulates the initiation and radial position of plant lateral organs. *Plant Cell* **12**: 507–518
- Reinhardt D, Pesce ER, Stieger P, Mandel T, Baltensperger K, Bennett M, Traas J, Friml J, Kuhlemeier C (2003) Regulation of phyllotaxis by polar auxin transport. *Nature* **426**: 255–260
- Roos MD, Hanover JA (2000) Structure of O-linked GlcNAc transferase: mediator of glycan-dependent signaling. *Biochem Biophys Res Commun* **271**: 275–280
- Sasaki A, Itoh H, Gomi K, Ueguchi-Tanaka M, Ishiyama K, Kobayashi M, Jeong D-H, An G, Kitano J, Ashikari M, et al (2003) Accumulation of phosphorylated repressor for gibberellin signaling in an F-box mutant. *Science* **299**: 1896–1898
- Scheufler C, Brinker A, Bourenkov G, Pegoraro S, Moroder L, Bartunik H, Hatl FU, Moarefi I (2000) Structure of TPR domain-peptide complexes: critical elements in the assembly of the Hsp70-Hsp90 multichaperone machine. *Cell* **101**: 199–210
- Shafi R, Iyer SP, Ellies LG, O'Donnell N, Marek KW, Chui D, Hart GW, Marth JD (2000) The O-GlcNAc transferase gene resides on the X chromosome and is essential for embryonic stem cell viability and mouse ontogeny. *Proc Natl Acad Sci USA* **97**: 5735–5739
- Sheffield VC, Beck JS, Kwitek AE, Sandstrom DW, Stone EM (1993) The sensitivity of single-strand conformation polymorphism analysis for the detection of single base substitutions. *Genomics* **16**: 325–332
- Silverstone AL, Ciampaglio CN, Sun T-p (1998) The Arabidopsis RGA gene encodes a transcriptional regulator repressing the gibberellin signal transduction pathway. *Plant Cell* **10**: 155–169
- Silverstone AL, Jung H-S, Dill A, Kawaide H, Kamiya Y, Sun T-p (2001) Repressing a repressor: gibberellin-induced rapid reduction of the RGA protein in Arabidopsis. *Plant Cell* **13**: 1555–1566
- Silverstone AL, Mak PYA, Casamitjana Martínez E, Sun T-p (1997) The new RGA locus encodes a negative regulator of gibberellin response in Arabidopsis thaliana. *Genetics* **146**: 1087–1099
- Singh DP, Jermakow AM, Swain SM (2002) Gibberellins are required for seed development and pollen tube growth in Arabidopsis. *Plant Cell* **14**: 3133–3147
- Slawson C, Hart GW (2003) Dynamic interplay between O-GlcNAc and O-phosphate: the sweet side of protein regulation. *Curr Opin Struct Biol* **13**: 631–636
- Sun T-p, Gubler F (2004) Molecular mechanism of gibberellin signaling in plants. *Annu Rev Plant Biol* **55**: 197–223
- Swain SM, Singh DP (2005) Tall tales from sly dwarves: novel functions of gibberellins in plant development. *Trends Plant Sci* **10**: 123–129
- Swain SM, Tseng T-s, Olszewski NE (2001) Altered expression of SPINDLY affects gibberellin response and plant development. *Plant Physiol* **126**: 1174–1185
- Swain SM, Tseng T-s, Thornton TM, Gopalraj M, Olszewski N (2002) SPINDLY is a nuclear-localized repressor of gibberellin signal transduction expressed throughout the plant. *Plant Physiol* **129**: 605–615
- Thomas SG, Sun T-p (2004) Update on gibberellin signaling: a tale of the tall and the short. *Plant Physiol* **135**: 668–676
- Thornton TM, Swain SM, Olszewski NE (1999) Gibberellin signal transduction presents...the SPY who O-GlcNAc'd me. *Trends Plant Sci* **4**: 424–428
- Tseng TS, Salome PA, McClung CR, Olszewski NE (2004) SPINDLY and GIGANTEA interact and act in Arabidopsis thaliana pathways involved in light responses, flowering, and rhythms in cotyledon movements. *Plant Cell* **16**: 1550–1563
- Tseng T-s, Swain SM, Olszewski NE (2001) Ectopic expression of the tetratricopeptide repeat domain of SPINDLY causes defects in gibberellin response. *Plant Physiol* **126**: 1250–1258

- Tyler L, Thomas SG, Hu J, Dill A, Alonso JM, Ecker JR, Sun T-p** (2004) DELLA proteins and gibberellin-regulated seed germination and floral development in *Arabidopsis*. *Plant Physiol* **135**: 1008–1019
- Tzamarias D, Struhl K** (1995) Distinct TPR motifs of Cyc8 are involved in recruiting the Cyc8-Tup1 corepressor complex to differentially regulated promoters. *Genes Dev* **9**: 821–831
- Ueguchi-Tanaka M, Ashikari M, Nakajima M, Itoh H, Katoh E, Kobayashi M, Chow TY, Hsing YI, Kitano H, Yamaguchi I, et al** (2005) *GIBBERELLIN INSENSITIVE DWARF1* encodes a soluble receptor for gibberellin. *Nature* **437**: 693–698
- Wells L, Vosseller K, Hart GW** (2001) Glycosylation of nucleocytoplasmic proteins: signal transduction and *O*-GlcNAc. *Science* **291**: 2376–2378
- Wen C-K, Chang C** (2002) *Arabidopsis RGL1* encodes a negative regulator of gibberellin responses. *Plant Cell* **14**: 87–100
- Wilson RN, Heckman JW, Somerville CR** (1992) Gibberellin is required for flowering in *Arabidopsis thaliana* under short days. *Plant Physiol* **100**: 403–408
- Wilson RN, Somerville CR** (1995) Phenotypic suppression of the gibberellin-insensitive mutant (*gai*) of *Arabidopsis*. *Plant Physiol* **108**: 495–502
- Young JC, Obermann WM, Hartl FU** (1998) Specific binding of tetratricopeptide repeat proteins to the C-terminal 12-kDa domain of hsp90. *J Biol Chem* **273**: 18007–18010
- Yu H, Ito T, Zhao Y, Peng J, Kumar P, Meyerowitz EM** (2004) Floral homeotic genes are targets of gibberellin signaling in flower development. *Proc Natl Acad Sci USA* **101**: 7827–7832